

Multi-wavelength digital holography for 3D-shape-measurements on rough surfaces

Markus Fratz, Daniel Carl, Danilo Skoczowski, Axel Heuer, Heinrich Höfler
 Fratz, Markus; Carl, Daniel; Skoczowski, Danilo; Heuer, Axel; Höfler, Heinrich;
 Fraunhofer Institute for Physical Measurement Techniques (IPM) / University of Potsdam, Institute for
 Physics and Astronomy, Chair of Photonics
 Heidenhofstraße 8, 79110 Freiburg, Germany / Karl-Liebknecht-Str. 24-25, 14476 Potsdam, Germany

Motivation

Fast and accurate measurement of the topography of technical surfaces is a demanding task in modern fabrication processes. For 100% inspection of typical mechanical components the data acquisition and evaluation has to be performed within a few seconds. Measurement volumes in the order of 10 mm x 20 mm x 20 mm with resolution in the micrometer range are desired, but they cannot be achieved within reasonable time scales using conventional approaches like e.g. white light interferometry or depth-from-focus systems. Digital holography is a promising technique for 3D measurements of technical surfaces.

Optical setup

We present a novel system that is capable of non-contact three-dimensional measurements based on lensless digital holography. Six separately stabilized laser diodes act as light sources. The laser light of each of the laser sources is coupled into a fiber-optical switch which allows for the selection of the actually used laser wavelength. The laser light is emitted into a digital holographic setup as shown in figure 1.

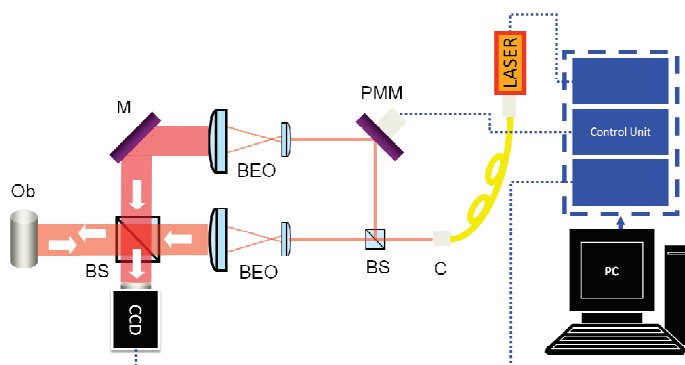


Figure 1 Schematic of the setup for the acquisition of on-axis digital holograms.
 C: Collimator; BS: beam splitter; BEO: beam expanding optics; M: Mirror; PMM: piezo-mounted mirror; Ob: Object under investigation

The light is collimated and divided into two beamlets by a polarizing beam splitter cube. The beamlet passing the beam splitter cube without deflection is expanded and illuminates the object under investigation. This beamlet is denoted as the object beam. The light diffracted by the object is directed onto a CCD-Camera (1000 x 1000 Pixels) by means of a second beam splitter cube. No objective lens is used for the image acquisition. The second beamlet, the reference beam, is expanded, too, and interferes with the object beam on the CCD-camera resulting in a digital hologram. The optical path length of the reference beam can be varied by means of a piezo actuator to shift the relative phase between object and reference beam.

For each of the six wavelengths three phase-shifted holograms are recorded. The phase steps introduced by the piezo actuator can be calculated from the holograms using a method proposed by Cai et al. [1]. The phase extraction method makes the image acquisition less sensitive to vibrations of the optical setup like e. g. relative movements of the object under investigation with respect to the optical setup. As a result of the phase shifting procedure the complex amplitude $A_{CCD}(x,y)$ of the object wave in the plane of the camera chip is determined for each of the six wavelengths.

To gain information about the three-dimensional shape of the object under investigation the complex amplitude in a plane close to the surface of the object has to be reconstructed. This can be achieved

using numerical methods that simulate the free space propagation of light. A well suited method is proposed in [2]. This method is especially appropriate for multi-wavelength holography due to the fact that the reproduction scale of the reconstructed wave at a given plane can be kept constant independent of the used wavelength of light. The numerical reconstruction results in the knowledge of the optical fields in a plane close to the surface of the object under investigation. To extract the 3D-information only the phase values $\phi_m(x,y)$ of the complex amplitude $A(x,y) = |A(x,y)|\exp(j\phi_m(x,y))$ in that plane are of interest. The index m denotes the respective wavelength while j is the complex unit. Those phase values depend on the height $h(x,y)$ of the object as follows:

$$h(x,y) = \frac{1}{2} \frac{\phi_m(x,y)}{2\pi} \lambda_m \quad [1]$$

The unambiguous measurement range for $h(x,y)$ is limited here by $\lambda/2$. To extend this range the difference between reconstructed phase values at slightly different wavelengths λ_m and λ_n can be used:

$$h(x,y) = \frac{1}{2} \frac{\phi_m(x,y) - \phi_n(x,y)}{2\pi} \frac{\lambda_n \lambda_m}{\lambda_m - \lambda_n} \quad [2]$$

Due to the similarity of equations [1] and [2] the term $\lambda_n \lambda_m / (\lambda_n - \lambda_m) = \lambda_{nm}$ is called artificial wavelength. The accuracy of the respective measured height values at different artificial wavelengths depends on the noise of the individual phase distributions $\phi_m(x,y)$ and $\phi_n(x,y)$ as well as on the accurate knowledge of the artificial wavelengths λ_{nm} and scales with the artificial wavelength. By combining the six phase distributions reconstructed at all the used wavelengths it is possible to gain height maps of the object at different axial resolutions and unambiguous measurement ranges. In a hierarchical process it is possible to use the large unambiguous measurement range that arises from the largest artificial wavelength ($\lambda_{01} \sim 22$ mm) with the high accuracy of height images at the smallest artificial wavelength ($\lambda_{05} \sim 185$ μm).

Results

Figure 2 illustrates the reconstructed complex amplitude of a typical technical surface. A photograph of the object is given in fig. 2 (e) and drawing illustrating the dimensions of the object is depicted in fig 2 (f). The images (a) and (b) correspond to the absolute values and phase distributions recorded and reconstructed at a wavelength of 635.808 nm, respectively. Images (c) and (d) depict the corresponding results for a second wavelength of 635.825 nm. It can be seen that the absolute values of the reconstructed complex amplitude contain information about the reflectivity of the object similar to a photographic image. The phase images can not be interpreted directly as height images because the rough surface of the object causes the appearance of speckles. By subtracting fig 2 (b) and (d) from each other it is nevertheless possible to get access to the height information contained in these images because the speckle fields at the slightly different wavelengths are correlated to each other [3].

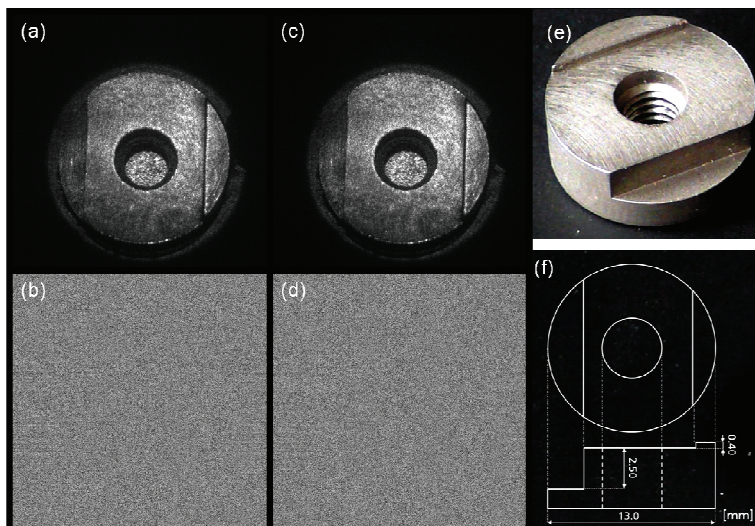


Figure 2 Complex Amplitudes at different wavelengths

- (a) Absolute values of reconstructed amplitude at $\lambda_m = 635.808$ nm
- (b) Phase values $\phi_m(x,y)$ at $\lambda_m = 635.808$ nm
- (c) Absolute values of reconstructed amplitude at $\lambda_n = 635.825$ nm
- (d) Phase values $\phi_n(x,y)$ at $\lambda_n = 635.825$ nm
- (e) Photograph of the investigated object
- (f) Drawing of the object

In the current setup six different wavelengths are used. From these wavelengths height images corresponding to artificial wavelengths ranging from 23.8 mm ($\lambda_m = 635.808$ nm, $\lambda_n = 635.825$ nm) down to 183 μm ($\lambda_m = 635.808$ nm, $\lambda_n = 636.999$ nm) are available.

A typical result of a complete measurement cycle is given in fig 3. In figure 3 (a) a measured height map of the object shown in figure 2 is given. The dark spots result from sampling points where not enough light from the object is collected and thus those sampling points are interpreted as invalid points. Fig 3 (b) depicts a 3D representation of the measured height distribution. Fig 3(c) shows a cross-section of the measured height distribution along the dotted line of fig 3 (a).

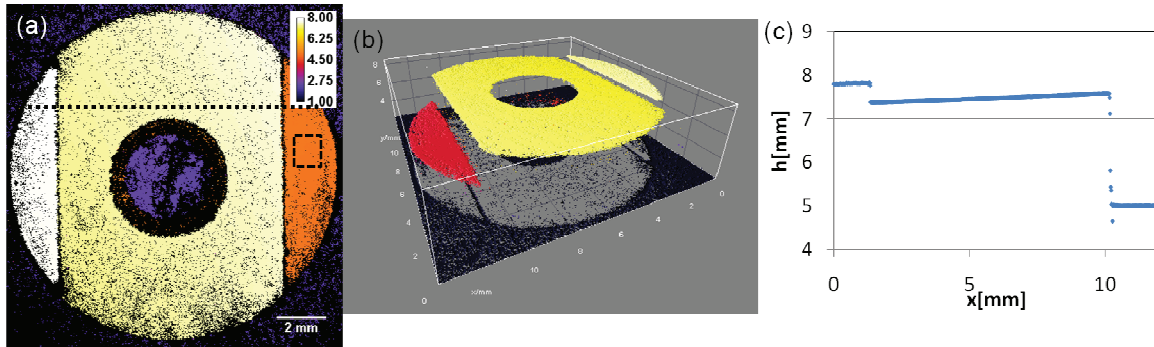


Figure 3 Measured shape of the object of fig 2

(a) Measured height map $h(x,y)$ of the object; unit of the calibration bar is mm

(b) Point-cloud representation of the measured height

(c) Cross-Section of the measured height along the dotted line of (a)

The shape of the object is exactly reproduced by our measuring system. To determine the measurement accuracy of our system the standard deviation of the measured values in the dashed square in fig 3 (a) was calculated. This region consists of 100 x 100 sampling points. The standard deviation of the measured values in this region was determined to be 3.98 μm .

References

1. L. Z. Cai, Q. Liu, and X. L. Yang, "Generalized phase-shifting interferometry with arbitrary unknown phase steps for diffraction objects", *Opt. Lett.* **29**, 183-185 (2004).
2. F. Zhang, I. Yamaguchi, and L. P. Yaroslavsky, "Algorithm for reconstruction of digital holograms with adjustable magnification," *Opt. Lett.* **29**, 1668-1670 (2004).
3. I. Yamaguchi, "Speckle Correlation in Phase-Shifting Digital Holography," in *Digital Holography and Three-Dimensional Imaging*, OSA Technical Digest (CD) (Optical Society of America, 2010), paper DMA2